

GALAXIES AT THE EXTREMES: ULTRA-DIFFUSE GALAXIES IN THE VIRGO CLUSTER

J. CHRISTOPHER MIHOS,¹ PATRICK R. DURRELL,² LAURA FERRARESE,³ JOHN J. FELDMEIER,²
PATRICK CÔTÉ,³ ERIC W. PENG,^{4,5} PAUL HARDING,¹ CHENGZE LIU,^{6,7}
STEPHEN GWYN,³ AND JEAN-CHARLES CUILLANDRE⁸

Draft version July 27, 2015

ABSTRACT

We report the discovery of three large ($R_{29} \gtrsim 1'$) extremely low surface brightness ($\mu_{V,0} \approx 27.0$) galaxies identified using our deep, wide-field imaging of the Virgo Cluster from the Burrell Schmidt telescope. Complementary data from the *Next Generation Virgo Cluster Survey* do not resolve red giant branch stars in these objects down to $i = 24$, yielding a lower distance limit of 2.5 Mpc. At the Virgo distance, these objects have half-light radii 3–10 kpc and luminosities $L_V = 2 - 9 \times 10^7 L_\odot$. These galaxies are comparable in size but lower in surface brightness than the large ultradiffuse LSB galaxies recently identified in the Coma cluster, and are located well within Virgo's virial radius; two are projected directly on the cluster core. One object appears to be a nucleated LSB in the process of being tidally stripped to form a new Virgo ultracompact dwarf galaxy. The others show no sign of tidal disruption, despite the fact that such objects should be most vulnerable to tidal destruction in the cluster environment. The relative proximity of Virgo makes these objects amenable to detailed studies of their structural properties and resolved stellar populations. They thus provide an important new window onto the connection between cluster environment and galaxy evolution at the extremes.

Subject headings: galaxies: clusters: individual (Virgo) — galaxies: evolution — galaxies: fundamental parameters — galaxies: structure

1. INTRODUCTION

Our view of galaxy populations in the universe continues to be shaped by observational selection effects, particularly that of limiting surface brightness (Disney 1976). In the field, low surface brightness (LSB) galaxies exist in significant numbers (e.g., McGaugh 1996), but were largely unnoticed until the CCD imaging surveys of the 1980s (see, e.g., Bothun et al. 1997). Recent observations have probed even deeper, to limiting surface brightnesses of $\mu_B \approx 28 - 30$ mag arcsec⁻², revealing galaxies of ever lower surface brightness. This was demonstrated most recently through deep wide-field imaging of the Coma Cluster (van Dokkum et al. 2015a; vD15a, Koda et al. 2015; K15), which found a population of large ($r_e = 2 - 5$ kpc; i.e., Milky Way-sized) and extremely diffuse galaxies with central surface brightnesses $\mu_{0,V} = 24 - 26$. These objects preferentially (but not exclusively) populate the cluster outskirts, with follow-up spectroscopy confirming that at least one is located within Coma (van Dokkum et al. 2015b; vD15b).

That such diffuse galaxies exist in a rich cluster like

Coma is a surprise. Because of their low densities and shallow potential wells, LSB galaxies should be most vulnerable to tidal perturbations as they move through the cluster, making their lifetimes very short (e.g., Moore et al. 1996). Repeated encounters with other galaxies and with the cluster potential can whittle away stars from these objects, feeding the diffuse intracluster light. Complete tidal disruption may leave behind their high density nuclei, leading to the formation of ultracompact dwarf galaxies (UCDs; Bekki et al. 2003; Pfeffer & Baumgardt 2013). How the large, diffuse galaxies in Coma can survive this dynamically harsh environment is unclear, suggesting either that they may be falling into the cluster for the first time, or extremely dark matter dominated systems and thus more robust against tidal perturbations.

Finding such systems in the nearby Virgo Cluster would be of particular interest, since they would be close enough ($d_{\text{Virgo}} = 16.5$ Mpc; Mei et al. 2007, Blakeslee et al. 2009) to resolve their stellar populations and study their structure in detail. Large LSBs in Virgo were first hinted at in photographic catalogs by Sandage & Binggeli (1984); deeper studies subsequently identified diffuse objects with $\mu_{0,V} = 24 - 26$ and sizes $r_e > 1$ kpc (Impey et al. 1988; Caldwell 2006), somewhat less extreme than the Coma objects. New deep imaging of Virgo by Mihos et al. (2005 and in preparation), as well as the *Next Generation Virgo Cluster Survey* (NGVS; Ferrarese et al. 2012), now allow us to search for systems at even lower surface brightness. Here we report the discovery of three large, extremely diffuse LSBs found in our deep Virgo imaging. With central surface brightnesses of $\mu_{0,V} \approx 27.0$ and sizes of $r_e = 3 - 10$ kpc, these objects are comparable in size to the vD15a Coma objects, but even lower in surface brightness. All three objects are located in the inner 0.5 Mpc of Virgo, well within the virial ra-

¹ Department of Astronomy, Case Western Reserve University, 10900 Euclid Ave, Cleveland, OH 44106, USA

² Department of Physics and Astronomy, Youngstown State University, Youngstown, OH 44555, USA

³ Herzberg Institute of Astrophysics, National Research Council of Canada, Victoria, BC V9E 2E7, Canada

⁴ Department of Astronomy, Peking University, Beijing 100871, China

⁵ Kavli Institute for Astronomy and Astrophysics, Peking University, Beijing 100871, China

⁶ Center for Astronomy and Astrophysics, Department of Physics and Astronomy, Shanghai Jiao Tong University, Shanghai 200240, China

⁷ Shanghai Key Lab for Particle Physics and Cosmology, Shanghai Jiao Tong University, Shanghai 200240, China

⁸ Canada-France-Hawaii Telescope Corporation, Kamuela, HI 96743, USA

dus ($R_{vir} = 1.55$ Mpc; McLaughlin 1999). With such extremely low surface brightnesses, and projected deep within the cluster potential, these objects give us an opportunity for up-close study of the lowest density galaxies found in the high density cluster environment.

2. DEEP SURFACE PHOTOMETRY

To search for ultra diffuse galaxies in Virgo, we use our deep Virgo imaging survey from CWRU’s Burrell Schmidt telescope (Mihos et al. 2005 and in preparation). This survey covers 15.1 (16.3) degree² down to a per-pixel limiting surface brightness of 29.0 (28.5) mag arcsec⁻² in B (V) with a pixel scale of $1.45''$ pixel⁻¹. Throughout the imaging a myriad of small LSB objects can be seen; however, our interest here was to find the most extreme objects with isophotal sizes of $R_{V,29} \gtrsim 1'$ and central surface brightnesses $\mu_{V,0} \gtrsim 26.5$. Because objects at such low surface brightness and large angular size typically contain many compact, high surface brightness contaminants (foreground stars and background galaxies), automated detection algorithms are extraordinarily difficult to employ, and often miss true objects while making false detections due to instrumental noise, scattered light, or diffuse galactic cirrus. Rather than using automated detection, two of us (J.C.M. & J.J.F.) each made visual searches of the imaging, independently identifying three of these extreme LSBs — two in the Virgo cluster core, approximately halfway between M87 and M86, and a third 2° south of M87, towards the M49 sub-cluster. Subsequent inspection of the deep NGVS imaging (Ferrarese et al. 2012) confirms all objects, providing deep u^*giz data⁹ with sub-arcsecond seeing.

Figure 1 shows the deep Burrell Schmidt and NGVS imaging of our extreme Virgo LSBs. The right panel shows the location of the objects within Virgo, taken from from Mihos et al. in preparation. The middle panels show the Schmidt imaging both at full resolution, and after masking discrete sources and median filtering in 9×9 pixel ($13'' \times 13''$) scales. The rightmost panels show expanded views of the NGVS imaging, similarly processed to $1''$ pixel⁻¹ scales. The objects are clearly visible in both datasets. While this paper focuses on the largest LSB objects, many more smaller objects exist throughout Virgo; one example can be seen in the middle panels directly east (left) of VLSB-A: a small LSB galaxy originally identified in NGVS imaging (Figure 15 of Ferrarese et al. 2012).

To extract surface brightness profiles of these sources, we first use IRAF’s `objmasks` task to mask the brightest of the compact sources in and around each object. The sources are likely background contaminants; NGVS imaging resolves many of them into background galaxies, and we detect no excess of compact sources over the surrounding field in either VLSB-A or -C (VLSB-B does appear to have a slight excess, discussed in §3). We then calculate surface brightness profiles using both the average and median pixel intensities as a function of radius (Figure 2). Using an average includes the light from the fainter unmasked sources, while a median essentially traces the diffuse light alone. We fit Sersic models to the

median surface brightness profiles; the fits are shown in Figure 2, and the derived structural parameters given in Table 1. Ellipticity estimates for VLSB-B and -C come from GALFIT modeling; VLSB-A is too low in surface brightness to yield a meaningful estimate. We report average $B - V$ colors for VLSB-A and -B, but cannot measure a color for VLSB-C as it falls outside the B imaging footprint of the Schmidt survey.

The derived properties given in Table 1 show that, like the extreme Coma LSBs (vD15a, Koda et al. 2015; K15), these objects are reasonably well characterized by exponential profiles ($n \sim 1.0$). They are large ($r_e = 40'' - 120''$, or 3-10 kpc at the Virgo distance), extremely low in central surface brightness ($\mu_{V,0} \gtrsim 26.5$), and fairly red ($B - V = 0.6 - 0.7$). A search for the galaxies in other datasets finds they are undetected both in deep 21-cm ALFALFA data (Haynes et al. 2011) and far-UV GALEX imaging; coupled with their diffuse nature and lack of strong H α emission (A. Watkins, private communication), this suggests they are not actively forming stars.

Figure 3 compares our VLSB objects to other stellar systems, including early type galaxies in the Virgo and Fornax clusters and the Local Group, as well as globular clusters (GCs) and UCDs in Virgo (see Ferrarese et al. 2012 for details of the data compilation). We also include the extreme LSB galaxies in Coma from vD15a. In this figure, the Coma LSBs merge smoothly onto the sequence for high surface brightness galaxies, while the extreme Virgo LSBs reported here populate the plot at the low surface brightness end (see also K15). In this magnitude range ($M_B = -12$ to -15), early-type cluster galaxies show a continuum in surface brightness, similar to the distribution of surface brightness in the field (McGaugh 1996). The lack of small ($r_e \lesssim 1$ kpc) LSB galaxies in this plot is a selection effect; in Coma, they fall below the spatial resolution of vD15a, while in Virgo our selection focused on large galaxies ($R_{29} \gtrsim 1'$). At $\langle \mu_B \rangle_e > 26$, smaller objects certainly exist; they are seen in the K15 Coma sample and likely make up a significant fraction of the small LSB objects visible in Virgo in the Schmidt and NGVS surveys. It’s clear from these studies that LSB galaxies are well-represented in cluster galaxy populations, once selection effects are factored in.

3. DISCRETE SOURCE IMAGING

The preceding discussion presumes the VLSB objects are in fact Virgo Cluster members. To rule out a more local distance, we used NGVS imaging to search for any resolved stellar populations (likely luminous RGB stars). We use the NGVS master catalog to extract deep g and i photometry for all sources located within each object’s R_{29} isophotal radius. Point sources were selected as outlined in Durrell et al. (2014): by defining a concentration index $\Delta i = i_4 - i_8$, the difference between the 4-pixel and 8-pixel diameter i aperture-corrected magnitudes, and identifying point sources as objects with $|\Delta i| < 0.10$. Only the i data was used to define point sources, as the NGVS i images were taken under the best seeing conditions.

In Figure 4 we plot i , ($g - i$) color-magnitude diagrams (CMDs) for all point sources with $18 < i < 24$ within each object. The faint magnitude cutoff lies ~ 1 mag above the S/N= 10 limit for NGVS i sources, while the bright limit is avoids saturated objects. We also overplot

⁹ All magnitudes have been corrected for foreground extinction (Schlegel et al. 1998), and NGVS magnitudes are given in the CFHT MegaCam system.

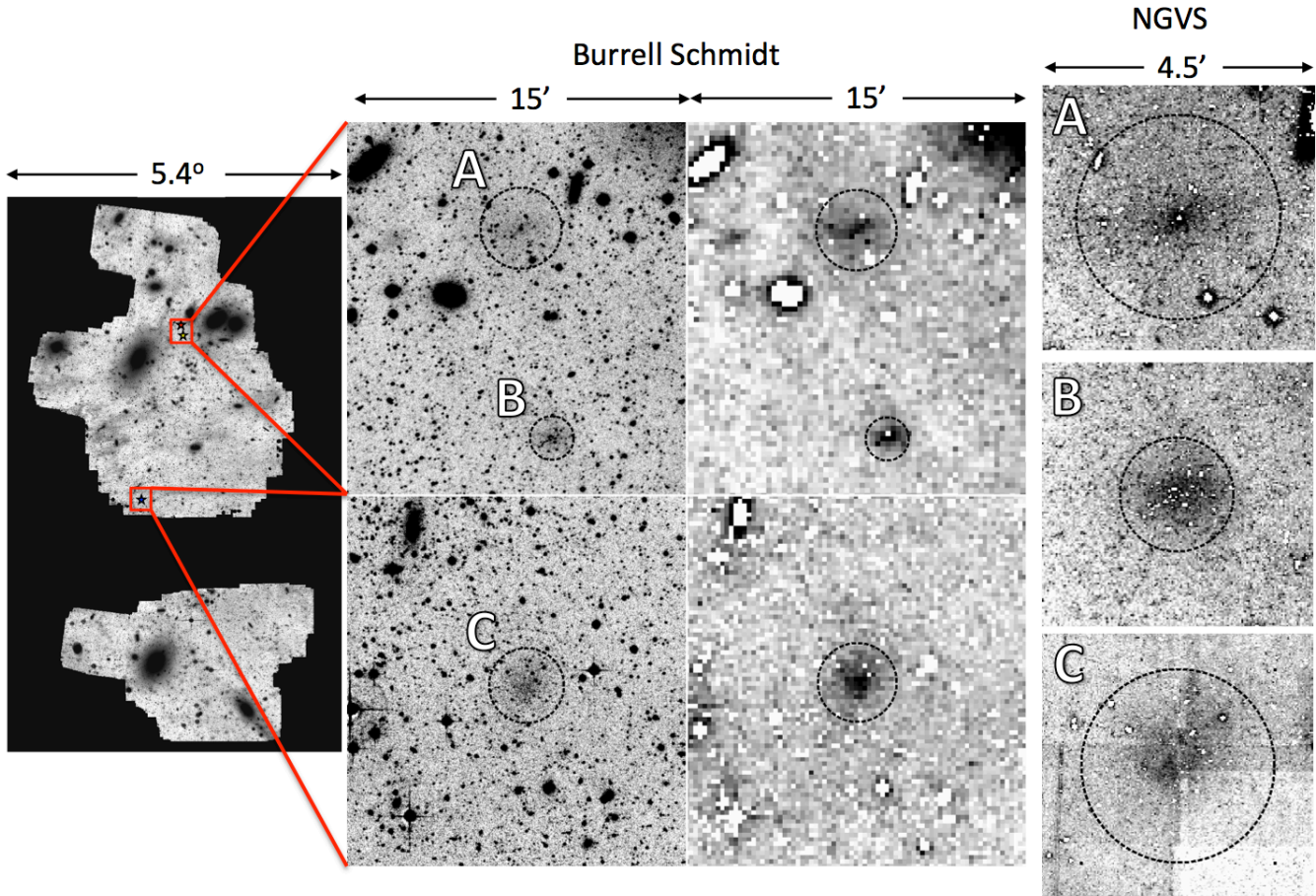


Figure 1. Optical imaging of the Virgo LSBs, with north up and east to the left. The leftmost panel shows objects’ locations within the full footprint of the Burrell Schmidt imaging survey, while the middle panels show the Schmidt imaging both at full resolution, and masked and rebinned to show faint structure. The rightmost panels show the NGVS imaging smoothed to $1''$ resolution.

the PARSEC isochrones of Bressan et al. (2012) with metallicities $Z = 0.00015$, $Z = 0.0015$ and $Z = 0.0060$ ($[M/H] = -2.0$, -1.0 , and -0.4 , respectively). We plot isochrones for a pair of distances: $d = 0.75$ Mpc, a representative Local Group distance, and $d = 2.5$ Mpc, the largest distance for which we could detect the most luminous RGB stars.

From the CMDs, we see no clear detection of any RGB population. For each isochrone distance, we can estimate the expected number of RGB stars by scaling the RGB population detected in a low luminosity ($M_V = -10.6$) Virgo dSph galaxy (Durrell et al. 2007). At 0.75 Mpc, we would expect 54, 21, and 96 RGB stars down to $i = 23.5$ in VLSB-A, -B, and -C respectively. At 2.5 Mpc, the expected RGB counts become 38, 15, and 66. Comparing these numbers to the paucity of the stellar sources along the RGB tracks shown in Figure 4, we conclude that all three of these objects must lie beyond 2.5 Mpc.

As a further check, Figure 4 also plots the radial number density profile of discrete sources (both resolved and point-like) within $3.5'$ of each object. If the VLSB objects are nearby, at $d < 2.5$ Mpc, their resolved stellar populations should appear as an increased density of point sources near the centers of each object. At Virgo-like distances, an excess of discrete sources near the galaxies would trace star clusters rather than individual stars,

Table 1
Extreme LSB Galaxies in Virgo^a

	VLSB-A ^b	VLSB-B	VLSB-C
RA	12:28:15.9	12:28:10.6	12:30:37.3
Dec	+12:52:13	+12:43:28	+10:20:53
R_{29}	$103'' (26'')$	$55'' (4'')$	$110'' (5'')$
$\mu_{V,0}$	27.0 (0.30)	26.7 (0.11)	26.7 (0.08)
$\langle \mu \rangle_{e,V}$	28.5 (0.30)	27.5 (0.11)	27.4 (0.08)
r_e	$121'' (24'')$	$36'' (2'')$	$69'' (3'')$
Sersic n	1.2 (0.22)	0.8 (0.08)	0.7 (0.05)
m_V	16.1 (0.53)	17.6 (0.16)	16.2 (0.11)
$(B - V)$	0.7 (0.1)	0.6 (0.1)	—
Ellipticity	—	0.17 (0.15)	0.12 (0.15)
M_V^c	-15.0	-13.5	-14.9
r_e^c	9.7 kpc	2.9 kpc	5.5 kpc

^a parameter uncertainties are shown in parentheses.

^b photometric properties for VLSB-A do not include its compact nucleus.

^c adopting $d_{\text{Virgo}} = 16.5$ Mpc.

while a lack of concentration would argue the sources are contaminants (predominantly background galaxies or foreground MW stars) unassociated with the VLSB objects entirely.

Figure 4 shows no excess of either point sources or resolved sources associated with VLSB-A or -C — the discrete sources are consistent with pure background

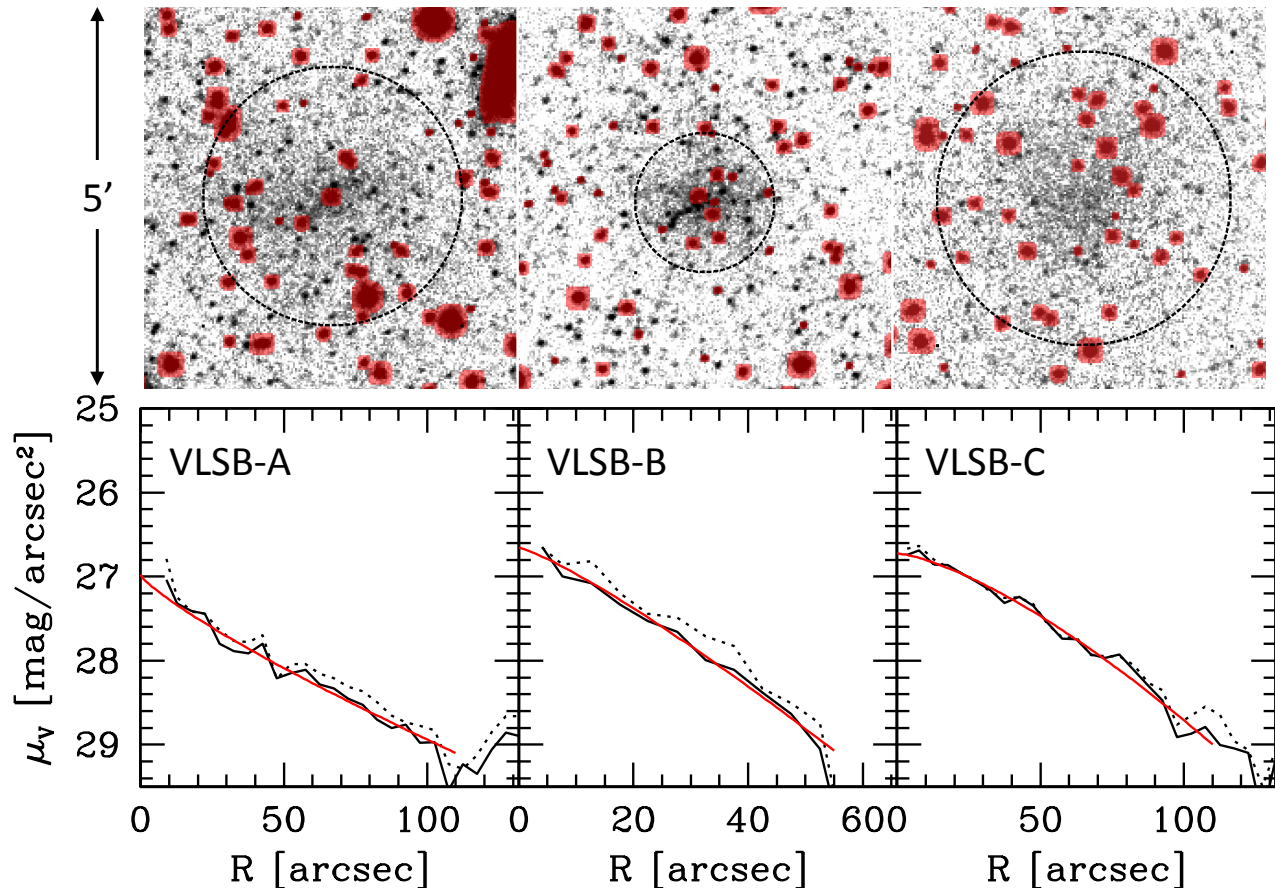


Figure 2. Surface photometry for the Virgo LSBs. Top: Schmidt imaging with photometry masks shown in red. Dashed circles show R_{29} for each galaxy. Bottom: Black curves show the average (dotted) and median (solid) surface brightness profiles; red curve shows Sersic fits to the median profiles.

contamination. Thus, VLSB-A and -C are indeed diffuse, with no sign of either resolved stars or star clusters. VLSB-B presents an interesting contrast, however, as we find an excess of both resolved sources and point sources within the galaxy. Several of these sources appear to be background galaxies, and the point source excess appears not to be resolved RGB stars, but rather a small population of globular clusters. We show this by also plotting in Figure 4 the density of sources with properties expected for Virgo globular clusters, using the selection criteria of Durrell et al. (2014): stellar or only slightly resolved sources ($-0.10 < \Delta i < 0.15$) with $0.55 < g - i < 1.15$ and $19.5 < i < 23.5$. We see a modest excess of these candidate globulars in VLSB-B, with $N = 6 \pm 3$ objects in the central $0.5'$, after removal of elongated objects (presumably background galaxies) and subtraction of a local background. This tentative detection of globular clusters supports the conclusion that VLSB-B is an extremely diffuse LSB galaxy located within Virgo.

4. NOTES ON INDIVIDUAL OBJECTS

VirgoLSB-A is projected deep within the Virgo core, 0.75° NW of M87 and 0.5° ESE of M86. It appears as a nucleated LSB galaxy with long, arcing tidal stream that runs NE-SW through the galaxy and extending off the frame in Figure 1 (the full extent of the stream can be seen in Figure 1 of Mihos et al. 2005). The tidal stream is curved concave to M86 (and to the nearby

galaxy pair NGC 4435/8), suggesting VLSB-A may be orbiting within the M86 subgroup rather than around M87 itself. The LSB component of the system is quite extended and shows a bar-like component oriented at 135° .

VLSB-A's nucleus is marginally resolved in our NGVS imaging; a structural analysis of the nucleus using KINGPHOT (Jordán et al. 2005, Liu et al. 2015) yields an effective radius of $r_{e,g} = 0.27''$ (22 pc). The nucleus has a radial velocity of -120 ± 40 km s $^{-1}$ (Peng et al. in preparation), quite distinct from M87 ($+1064$ km s $^{-1}$) and offset by $\sim 2\sigma_v$ from the mean velocity of Virgo E/S0 galaxies ($\langle v \rangle = 1017$ km s $^{-1}$, $\sigma_v = 589$ km s $^{-1}$; Binggeli et al. 1993). However, its similarity in velocity to M86 (-224 km s $^{-1}$), again argues that VLSB-A is part of Virgo's M86 subgroup.

On the whole, the properties of VLSB-A clearly suggest we are witnessing the dynamical formation of a new cluster UCD, made via tidal thrashing of a low mass cluster galaxy (e.g., Bekki et al. 2003; Pfeffer & Baumgardt 2013). The tidal stream and bar-like morphology of the galaxy are consistent with the response of a low mass galaxy to a strong tidal field, while the galaxy's red $B - V$ color suggests that star formation in the system has ceased. Figure 3 compares the structural properties of the nucleus of VLSB-A to UCDs in the Virgo core (Zhang et al. 2015, Liu et al. 2015), where it can be seen

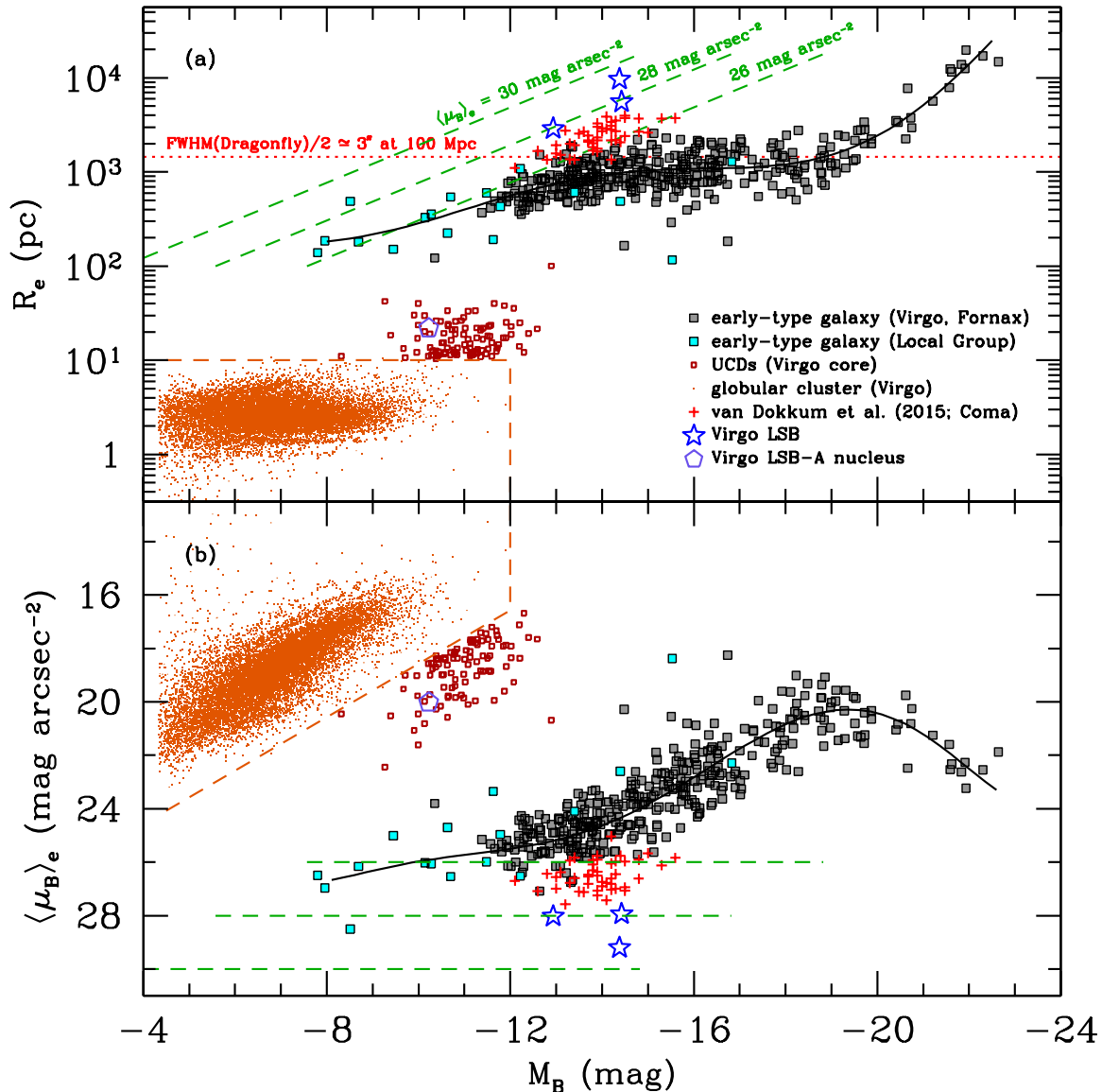


Figure 3. Structural properties of the Virgo LSBs compared with other stellar systems, including early type galaxies in the Virgo and Fornax Clusters and in the Local Group, as well as GCs and UCDs in Virgo, and the extreme LSBs found in Coma. The dashed orange lines show the GC selection box, while lines of constant surface brightness are shown in green.

that the nucleus lies in the large, low surface brightness tail of the UCD distribution. VLSB-A is likely in a short-lived transitory phase, as the cluster environment strips its diffuse outskirts to form a new Virgo UCD.

VirgoLSB-B is also projected onto the cluster core, only $9'$ south of VLSB-A. However, unlike VLSB-A it shows a more regular morphology with no obvious tidal debris, and is somewhat bluer ($B - V = 0.6$) as well. As noted previously, this object shows a significant population of sources photometrically consistent with Virgo globular clusters. Adopting a Gaussian globular cluster luminosity function with a turnover at $g_{\text{TO}} = 23.8 \pm 0.2$ and $\sigma = 1$ mag (Jordán et al. 2007), the total inferred GC population is $N_{\text{GC,tot}} = 9 \pm 4.5$. This yields a specific frequency of $S_N = 40 \pm 20$, rather large (albeit with large uncertainties) for galaxies of this luminosity, which typically have $S_N = 10 - 20$ with large spread (Peng et al. 2008, Georgiev et al. 2010).

Finally, **VirgoLSB-C** is found 2° (575 kpc or \sim

$\frac{1}{3}R_{\text{vir}}$) south of M87, between the Virgo A and M49 sub-clusters. The object appears to be purely diffuse, with no excess of compact sources over background in the system, and shows no obvious sign of tidal stripping.

5. DISCUSSION

The three objects presented here are quite diverse in their physical properties. While they are all large and extremely diffuse, and projected deep within Virgo, only one (VLSB-A) shows obvious signs of the tidal damage expected for diffuse galaxies in a dense environment; the other two are quite round ($\epsilon < 0.2$) with no morphological deformation or extended tidal debris. Meanwhile, globular clusters are only detected within VLSB-B, which suggests a surprisingly high specific frequency; neither VLSB-A or -C show evidence for globular clusters, yielding upper limits of $S_N \lesssim 2-3$ for these objects.

The differences between the objects may be due to differences in their evolutionary state or local environment. The tidal morphology of VLSB-A, along with its kine-

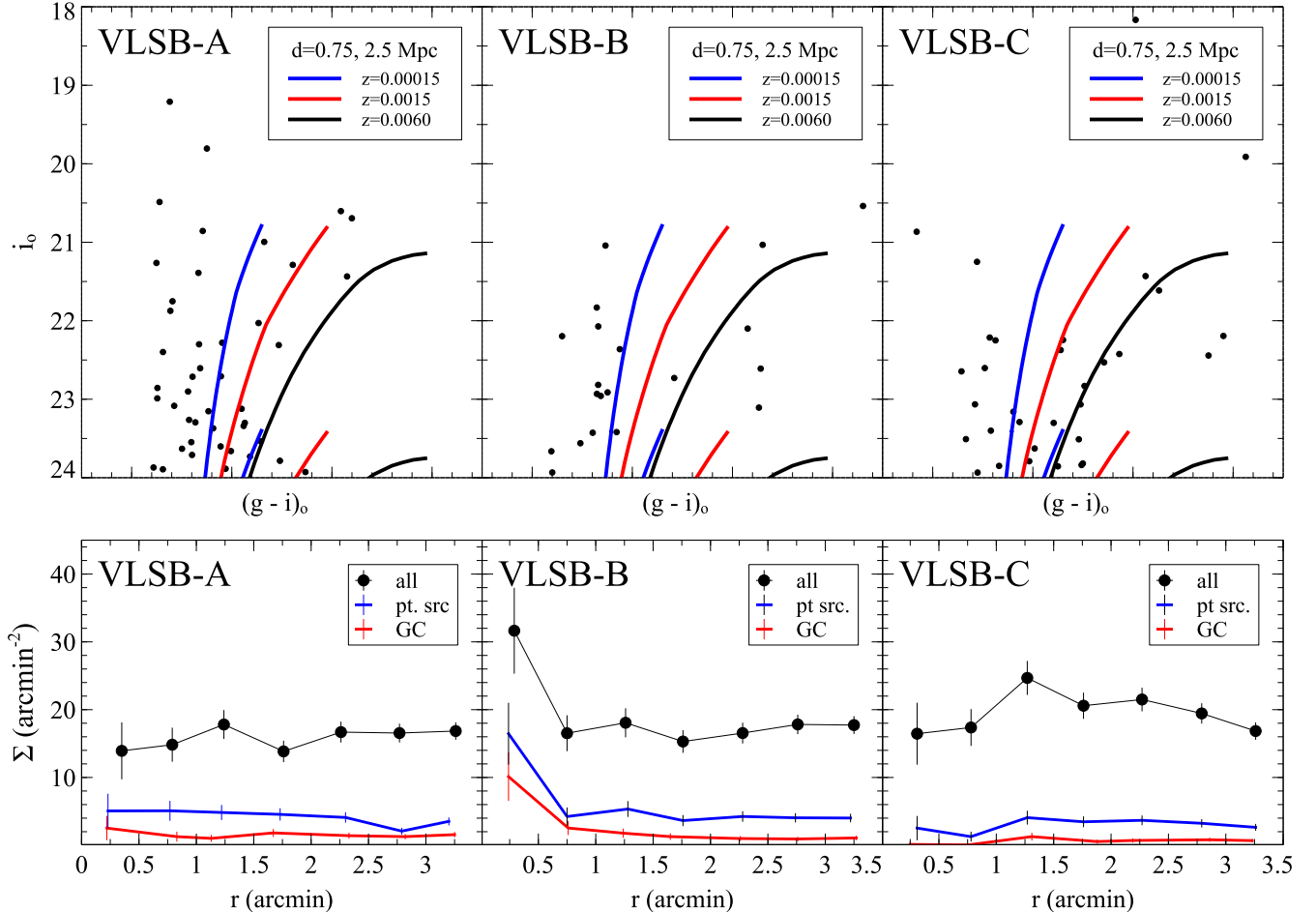


Figure 4. Photometry of discrete sources from NGVS imaging. Top: CMDs for point sources within each object, with RGB isochrones at $d=0.75$ and 2.5 Mpc overplotted for different metallicities. Bottom: radial density profiles for all discrete sources (black), point sources (blue), and sources photometrically consistent with Virgo globular clusters (red).

matic association with M86, strongly argues that the object is interacting within Virgo’s M86 subgroup. However, the lack of obvious tidal distortion in VLSB-B and -C, diffuse galaxies which should be most vulnerable to cluster tides, suggests instead they may lie in the cluster outskirts, or be falling into Virgo for the first time. Alternatively, they may be very dark matter dominated, like field LSBs (e.g., de Blok & McGaugh 1997), and therefore more resistant to tidal stripping. In this context, it is interesting that VLSB-B shows evidence for globular clusters. If globular cluster populations trace the dark matter content of a galaxy (e.g., Blakeslee et al. 1997; Peng et al. 2008; Harris et al. 2013; Hudson et al. 2014), the high specific frequency we infer for VLSB-B may be a signature of a massive dark halo that protects the system from rapid tidal destruction. However, a detailed understanding of how these objects fit into the picture of dynamically-driven galaxy evolution in clusters demands a better determination of both their local environment and their intrinsic properties.

While the properties of VLSB-A convincingly place it deep within Virgo, the situation for VLSB-B and -C is less clear. Without direct distance estimates (such as from the TRGB), our results do not unambiguously locate the objects within Virgo. While we rule out a Local Group distance, they may lie in the field along the line of

sight, either in front of or beyond Virgo. However, arguments that these are field objects merely projected onto the Virgo Cluster also run into problems, since their gas-poor nature and lack of knotty structure makes them very different from known field LSBs (e.g., de Blok & McGaugh 1997). Furthermore, if the objects lie beyond Virgo, their physical properties would be even more extreme — larger and more luminous (at fixed low surface brightness), potentially rivaling giant LSB galaxies such as Malin 1. Even if located in the intervening field, at distances 2.5 – 15 Mpc, their large angular sizes and low surface brightnesses show they still inhabit regions of structural parameter space that have been largely unexplored.

Nonetheless, the properties of VLSB-A, and the projection of all three galaxies well within Virgo’s virial radius, argue that they are indeed associated with the Virgo itself. The presence of extremely diffuse galaxies in Virgo (this paper) and Coma (vD15ab, K15) shows these objects populate a range of cluster environments. While ultradiffuse Coma galaxies have been reported in greater numbers than identified here, several factors make direct comparison difficult. First, our Schmidt imaging covers only the inner $\sim 15\%$ of Virgo; correcting for survey area suggests a total of ~ 20 objects throughout the cluster, and even more if they are located preferentially in the

cluster outskirts (as found in Coma; vD15a). Second, very few of the reported Coma objects approach the low surface brightnesses of our VLSB objects (see Figure 3); such systems may simply be intrinsically rare in *both* clusters. Finally, Coma is a much richer cluster than Virgo, and may house more galaxies of *all* types, LSBs included. However, in comparing LSB populations, cluster richness is a double-edged sword: a richer cluster may also make for a harsher dynamical environment that shortens their lifetime and reduces their overall numbers.

Ultimately, these questions will be best addressed through a cluster-wide census of the Virgo LSB galaxy population using wide-field surveys such as the NGVS. Identifying a larger sample of ultradiffuse galaxies in Virgo would also allow for detailed studies of their resolved stellar populations and physical structure on spatial scales not possible in more distant clusters. Thus a more systematic search for this elusive galaxy population in Virgo is well-motivated.

REFERENCES

- Bekki, K., Couch, W. J., Drinkwater, M. J., & Shioya, Y. 2003, MNRAS, 344, 399
- Binggeli, B., Popescu, C. C., & Tammann, G. A. 1993, A&AS, 98, 275
- Blakeslee, J. P., Jordán, A., Mei, S., et al. 2009, ApJ, 694, 556
- Bothun, G., Impey, C., & McGaugh, S. 1997, PASP, 109, 745
- Bressan, A., Marigo, P., Girardi, L., et al. 2012, MNRAS, 427, 127
- Côté, P., Blakeslee, J. P., Ferrarese, L., et al. 2004, ApJS, 153, 223
- Caldwell, N. 2006, ApJ, 651, 822
- de Blok, W. J. G., & McGaugh, S. S. 1997, MNRAS, 290, 533
- De Lucia, G., & Blaizot, J. 2007, MNRAS, 375, 2
- Disney, M. J. 1976, Nature, 263, 573
- Durrell, P. R., Côté, P., Peng, E. W., et al. 2014, ApJ, 794, 103
- Durrell, P. R., Williams, B. F., Ciardullo, R., et al. 2007, ApJ, 656, 746
- Ferrarese, L., Côté, P., Cuillandre, J.-C., et al. 2012, ApJS, 200, 4
- Gavazzi, G., Donati, A., Cucciati, O., et al. 2005, A&A, 430, 411
- Georgiev, I. Y., Puzia, T. H., Goudfrooij, P., & Hilker, M. 2010, MNRAS, 406, 1967
- Haegán, M., Jordán, A., Côté, P., et al. 2005, ApJ, 627, 203
- Haynes, M. P., Giovanelli, R., Martin, A. M., et al. 2011, AJ, 142, 170
- Hudson, M. J., Harris, G. L., & Harris, W. E. 2014, ApJ, 787, L5
- Impey, C., Bothun, G., & Malin, D. 1988, ApJ, 330, 634
- Jordán, A., Blakeslee, J. P., Côté, P., et al. 2007, ApJS, 169, 213
- Jordán, A., Côté, P., Blakeslee, J. P., et al. 2005, ApJ, 634, 1002
- Jordán, A., McLaughlin, D. E., Côté, P., et al. 2007, ApJS, 171, 101
- Jordán, A., Peng, E. W., Blakeslee, J. P., et al. 2009, ApJS, 180, 54
- Koda, J., Yagi, M., Yamanoi, H., & Komiyama, Y. 2015, arXiv:1506.01712
- McGaugh, S. S. 1996, MNRAS, 280, 337
- McGaugh, S. S., & de Blok, W. J. G. 1997, ApJ, 481, 689
- McLaughlin, D. E. 1999, ApJ, 512, L9
- Mei, S., Blakeslee, J. P., Côté, P., et al. 2007, ApJ, 655, 144
- Mihos, J. C., Harding, P., Feldmeier, J., & Morrison, H. 2005, ApJ, 631, L41
- Moore, B., Katz, N., Lake, G., Dressler, A., & Oemler, A. 1996, Nature, 379, 613
- Peng, E. W., Jordán, A., Côté, P., et al. 2008, ApJ, 681, 197
- Pfeffer, J., & Baumgardt, H. 2013, MNRAS, 433, 1997
- Sandage, A., & Binggeli, B. 1984, AJ, 89, 919
- van Dokkum, P. G., Romanowsky, A. J., Abraham, R., et al. 2015, ApJ, 804, L26
- van Dokkum, P. G., Abraham, R., Merritt, A., et al. 2015, ApJ, 798, L45
- Zhang, H.-X., Peng, E. W., Côté, P., et al. 2015, ApJ, 802, 30